

Chaotic Characteristic of Corona Discharge Series in Air Described by a 2D-nonlinear Discrete Dynamic Model

Abstract. In order to investigate the chaos characteristics of corona discharge current pulse series in air, the statistical distributions of points $(qn, \Delta tn+1)$ and points $(qn, \Delta tn, qn+1)$ were plotted and compared under different experimental conditions including applied voltage value, gap distance and curvature radius of positive point, etc. To describe and study this phenomenon in view of non-linear dynamics, a 2-dimensional nonlinear discrete dynamic model was built. The equation forms and its specific coefficients of the model were obtained by fitting method. The basic dynamic characteristics including the Eigenvalue of the linear matrix- λ (Lyapunov exponent) and the attractors were calculated and analyzed. And then, the output q-t series of the model at three different modulus of Lyapunov exponent were simulated and discussed. As a conclusion, it was suggested that the randomness and statistical feasibility of corona discharge series were greatly influenced by external experiment conditions and the stochastic corona time series in limited time scope could be interpreted as a phenomenon driven by chaos.

Streszczenie. W artykule zaprezentowano nową metodę statystycznej charakterystyki wyładowań koronowych występujących seryjnie. Opracowany został dwuwymiarowy model dynamiczny zjawiska, na podstawie którego wyznaczono i poddano analizie charakterystyki dynamiczne oraz kryteria teorii chaosu dotyczące wyładowań koronowych. (Charakterystyka chaotyczności seryjnych wyładowań koronowych w powietrzu na podstawie dwuwymiarowego, dyskretnego modelu dynamicznego)

Keywords: positive corona discharge; nonlinear dynamics; chaos; discharge series.

Słowa kluczowe: Dodatnie wyładowanie koronowe, dynamika nieliniowa, chaos, wyładowanie seryjne.

Introduction

Corona discharge is a kind of electrical discharge occurring with ionization in high electrical field. It has attracted extensive attentions for its destructive characters and its applications in many industrial fields, e.g., insulation diagnosis [1], electrochemistry [2], electro photography [3] and printing [4]. Until now, there are lots of studies on corona discharge [5-7], such as Loeb and Kip [8] and Fitzsimmons [9] on positive point corona in air, Trichel [10] and Loeb et al [11] on negative point corona in air, Ijumba et al [12] on energy loss of corona discharges. However, these studies mainly focus on mechanism and the macroscopic behaviors of corona discharge and are hard to explain or describe the stochastic appearance of corona discharge series. In recent years, with the development of nonlinear dynamics, some researchers have begun to study the nonlinear dynamic characteristics of corona discharge and other PD types, e.g., Dissado L A et al [13] proposed a nonlinear dynamic model for branched structures in the electrical breakdown of solid polymeric dielectrics; Tan X Y et al [14] analyzed the chaotic characteristic of the external circuit with a needle-plane corona defect; Luo Y F et al [15] tried to use the chaotic mathematics for PD recognition in Oil-Paper insulation. But till now, no much attention was paid to the chaotic and fractal behaviors of corona discharge. In addition, due to the randomness showed by the corona discharge, the internal non-stochastic components are often neglected. In this paper, a special experiment setup is used to get the data of q-t discharge current pulses. A new statistical method is proposed to obtain the statistical characteristic of the corona discharge time series, and then a 2D nonlinear dynamic model is established. Based on the proposed model, the dynamic characteristics and the chaotic criteria of corona discharge have been analyzed, which may help to understand the stochastic behaviors in corona discharge in terms of dynamics perspective.

The basic chaos theory

Chaos theories describe the erratic behavior in certain nonlinear dynamical systems, which study the behavior of dynamical systems that are highly sensitive to initial conditions. Small differences in initial conditions yield widely

diverging outcomes for chaotic systems, rendering long-term prediction impossible in general. The chaotic systems have the random-like behaviors in a limited time scope which are not driven by random factors. Explanation of such behaviors may be sought through analysis of a chaotic mathematical model, or through analytical techniques such as recurrence plots and Poincare maps. If we use discrete difference equations to describe chaotic systems, its characteristic could be obtained by means of iteration of discrete series. For instance, in N-dimension discrete dynamic system, the i-th value could be calculated by $x_i = f_i(x_0)$ (where $f(x_n)$ is a mapping from R^n (N-dimension real space) to R^n , x_0 is the initial value.) after the i-th iterations.

A. Criterion of chaos:

For N-dimensional mapping $\{x(i), i=1, 2, \dots, N\}$, by superimposing an infinitesimal arbitrary perturbations $dx(i)$ to the value of m moment $x_m(i)$, a new condition could be built up as:

$$(1) \quad x'_m(i) = x_m(i) + dx(i)$$

In this iteration system, $dx_n(i)$ is the difference between $\{x_{m+n}(i)\}$ and $\{x'_{m+n}(i)\}$. Its Maximal Lyapunov Exponent (MLE) is given by:

$$(2) \quad \lambda_{\max} = \lim_{N \rightarrow \infty} \frac{1}{N} \sum_{n=1}^N \log \frac{\|dx_n\|}{\|dx_{n-1}\|}$$

$$\text{where: } \|dx_n\| = \sqrt{\sum_{i=1}^L [dx_n(i)]^2}$$

Lyapunov Exponent spectrum can be calculated by Gram-Schmitor thogonalization method (also called linearization matrix method). For instance, there is a first order differential equations set with two dimensions, as shown in following:

$$(3) \quad \begin{cases} x = f(x, y) \\ y = g(x, y) \end{cases}$$

where f and g are the nonlinear functions of x and y , respectively.

Equation (4) is the slope of each point along the phase trace on the phase plane except for the equilibrium points.

$$(4) \quad \frac{dy}{dx} = \frac{g(x, y)}{f(x, y)}$$

By introducing two variables η and ξ nearby the equilibrium points and making $x=x_0+\eta$, $y=y_0+\xi$, the linear result for the equilibrium points can be obtained by:

$$(5) \quad \begin{pmatrix} \dot{\eta} \\ \dot{\xi} \end{pmatrix} = \begin{pmatrix} \frac{\partial f}{\partial x} & \frac{\partial f}{\partial y} \\ \frac{\partial g}{\partial x} & \frac{\partial g}{\partial y} \end{pmatrix} \begin{pmatrix} \eta \\ \xi \end{pmatrix} = M \begin{pmatrix} \eta \\ \xi \end{pmatrix}$$

Stability solution of equations (also called fixed points) is determined by the modulus of Eigenvalue, $\lambda_{1,2}$. When $|\lambda_{1,2}| < 1$, the fixed point is convergent; When $|\lambda_{1,2}| > 1$, it is unstable.

B. Discussion about systematicness and randomness of corona discharge series:

Generally, it is difficult to distinguish whether the signal of corona discharge series is a pure random behavior or chaotic behavior because the deterministic chaotic dynamical system also has some "random-like" features in a finite time scope. From a physical point of view, the corona discharge series are determined by mutual constraint and influence of the factors, such as production of initial effective electrons, electric field distortion by bifurcate of streamer and the memory effect of discharge channel. These complex physical motivations constitute a dynamic system which may have some chaotic characteristics.

2D nonlinear discrete dynamic model of corona discharge series

Some researchers have studied the q - t characteristic of corona discharge current and proposed some models [16]. In Fromm's study, a model called "Time lag/Recovery model" for PD recognition has been verified experimentally for void discharge and point corona discharge, as shown in Fig.1., where q_{n-1} , q_n and q_{n+1} are the magnitudes of $(n-1)$ -th discharge, n -th discharge and $(n+1)$ -th discharge, respectively, $\Delta t_{pre(n)}$ and $\Delta t_{suc(n)}$ are the current time lag and the previous time lag of n -th discharge, respectively.

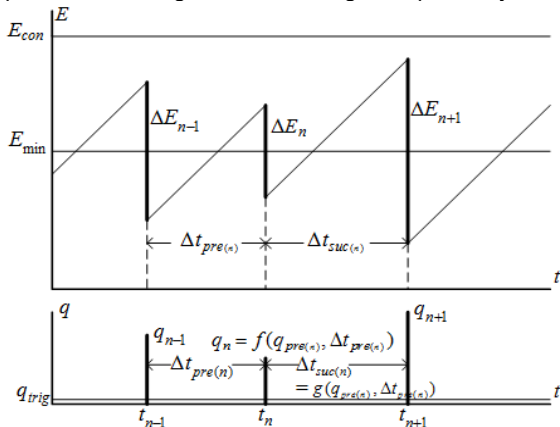


Fig.1. Demonstration of time lag/recovery model

Time lag/Recovery model was presented for PD recognition under the assumption that the discharge current magnitude was related to the previous time-lag but was not depended on the last discharge magnitude. In fact, according to some researchers' studies [17,18], the last discharge has some effect on the current discharge through the influences such as the space charge distributing in residual channel, the electron energy and the recovering of

internal electric field. Therefore, at the micro level, each corona pulse is depended by not only the time lag but also the precious discharge quantity (or magnitude). Based on this theory, 2D functions could be built as the form:

$$(6) \quad \begin{cases} q_{suc(n)} = f(q_{pre(n)}, \Delta t_{pre(n)}), \\ \Delta t_{suc(n)} = g(q_{pre(n)}) \end{cases}$$

Let $q_{n+1}=q_{suc(n)}$, $q_n=q_{pre}$, $\Delta t_{n+1}=\Delta t_{suc}$, $\Delta t_n=\Delta t_{pre}$, a discrete dynamic model can be built up as the form:

$$(7) \quad \begin{cases} q_{n+1} = f(\Delta t_n, q_n), \\ \Delta t_{n+1} = g(q_n) \end{cases}$$

Experiment and mathematical model of corona in atmosphere air

A. Experimental setup:

In order to obtain the expression form of function (7) and its specific coefficients, an experimental setup has been developed to obtain the data of q - t of corona discharge, as shown in Fig. 2. The corona discharge is generated by a positive point to plane electrode in air. The curvature radius of the point is about $50\mu\text{m}$. HVDC voltage is applied to the point electrode and the plane electrode is grounded. The grounding wire is surrounded by an inductively-coupled compensated Rogowski coil (IPC CM-100-L) with bandwidth from 30kHz to 140MHz and sensitivity 5.5VA-1 for 20ns pulsewidth. A 50Ω non-inductive measurement resistance is also used to obtain the corona pulses. The digital oscilloscope (Lecroy 64MXs-B) with 600MHz response bandwidth and 10Gs/s sampling rate is also used to observe the corona discharge while the data of magnitude of pulse q and the time lag Δt are collected by a high speed acquisition (125MS/s, 14bit) and stored by a Peak-hold recorder.

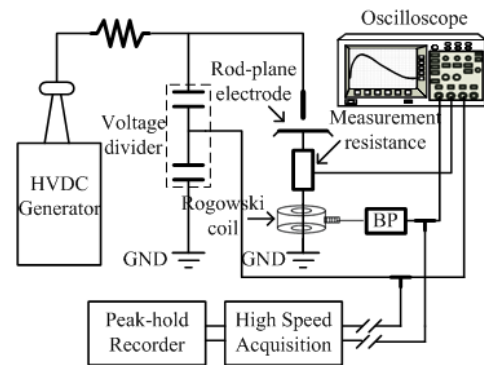


Fig.2. The schematic of experimental setup

B. Determination of specific form and its parameters of the 2D nonlinear discrete dynamic model:

According to statistical analysis of experimental data (q - t) collected by the recorder, the specific form and its parameters of the corona discharge time series model aforementioned in Sec.3 could be established by fitting points $(q_n, \Delta t_{n+1})$ and points $(q_n, \Delta t_n, q_{n+1})$ in coordinate system. In this study, it is observed that a tiny perturbation of experimental condition would cause a chain of events leading to large-scale difference in the statistical result. That means that the distributions of points $(q_n, \Delta t_{n+1})$ and points $(q_n, \Delta t_n, q_{n+1})$ in the coordinates sometimes are concentrated (which could be used as the valid data in fitting) and sometimes are very decentralized without obvious statistical correlation. Therefore corona time series could be evolved from ordered and stable to unordered and unstable under some particular condition, or be changed in opposite process. Two actual pulse current waveforms under similar

experiment conditions obtain by oscilloscope are showed in Fig. 3(a) and (b). In appearance, both of the corona discharge pulses under condition a. and b. have no obvious regular pattern. But the distributions of the pulse series of the former is more concentrated than the latter, as shown in Fig.4(a).

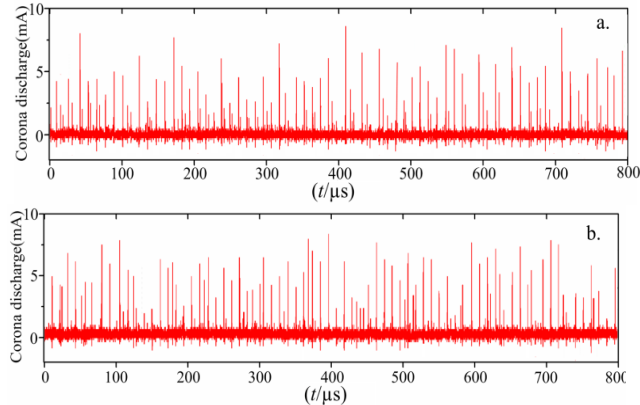
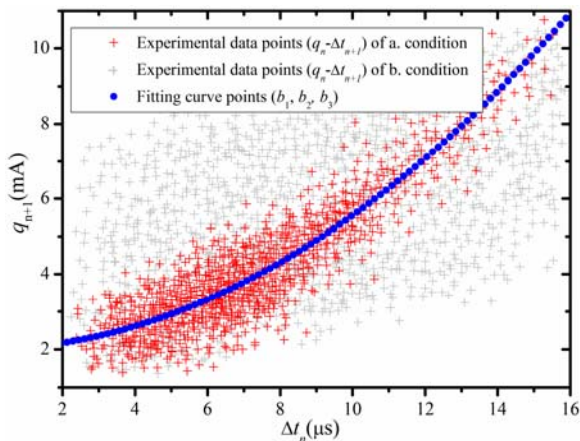


Fig.3. Corona discharge current pulse series under different experimental condition
a. gap distance $d=8\text{mm}$, curvature radius $r=50\mu\text{m}$, applied voltage value $=10\text{kV}$, air pressure $=0.1\text{MPa}$;
b. gap distance $d=15\text{mm}$, curvature radius $r=50\mu\text{m}$, applied voltage value $=15\text{kV}$, air pressure $=0.1\text{MPa}$.

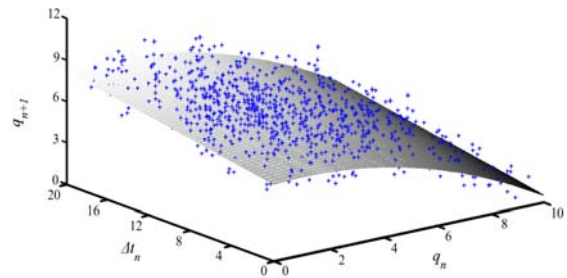
The expressions of function (7) could be obtained by iterative fitting the valid $q-t$ data. Linear regression goodness of fit tests is performed on the iteration. The optional polynomial order is selected through the test of the partial fitting square sum on the basis of the variance of the fitting equation, and the second-order polynomial (parabola) is determined. The specific parabola form is shown in (8). The expressions of f and g have the same maximum order, and Δt_n is a proportion term in the function $f(\Delta t_n, q_n)$.

$$(8) \quad \begin{cases} q_{n+1} = a_1 q_n^2 + a_2 q_n + a_3 \Delta t_n + a_4 \\ \Delta t_{n+1} = b_1 q_n^2 + b_2 q_n + b_3 \end{cases}$$

Taking "a. condition" aforementioned as an example, for obtaining accurate coefficients, it needs enough data points to ensure the Standard Error (S.E. <0.1) and the Coefficient of Determination (Adj. R square $=1-\text{SSE}/\text{SST}<1$) within the acceptable error limits. The experiment data points distributions $(q_n, \Delta t_{n+1})$ and $(q_n, \Delta t_n, q_{n+1})$, and the fitting curves are presented in coordinates, as shown in Fig. 4. The fitting results of coefficients are listed in the Table 1. The Adj. R Square of fitting expressions f and g are 0.853 and 0.722, respectively.



(a) $q_n-\Delta t_{n+1}$



(b) $q_n-\Delta t_n-q_{n+1}$
Fig.4. Distributions of points $(q_n, \Delta t_{n+1})$ and points $(q_n, \Delta t_n, q_{n+1})$

Chaotic characteristics of the 2D nonlinear discrete dynamic model

Chaos is disorder state of nonlinear dynamic system which is determined by some mathematical criteria. In order to analyze the chaotic characteristics of the corona discharge model, the following points have been discussed: 1) Maximal Lyapunov Exponent (MLE) and the simulations at different MLE; 2) Bifurcations caused by change of parameters of the model; 3) Attractors of the model system and the sensitivity to initial conditions.

A. MLE of the model system :

The stabilities of the fixed points $x_{0,1}$ in the iterative functions should be firstly considered for investigation of dynamic characteristic of corona discharge. The fixed points $x_{0,1}$ can be obtained by solving the equation when $F(x)=0$:

$$(9) \quad F(x_{n-1}, x_n, x_{n+1}) = \alpha x^2 + \beta x + \gamma = 0$$

$$(10) \quad \begin{cases} x_{0,1} = \frac{1}{2\alpha} [-\beta \pm (\beta^2 - 4\alpha\gamma)^{1/2}] \\ y_{0,1} = g(x_{0,1}) \end{cases}$$

where: $\alpha=a_1+b_1$, $\beta=a_2+a_3b_2$, $\gamma=a_4+a_3b_3$.

The Lyapunov Exponent (λ) can be calculated by linear matrix method (in Sec.2.1):

$$(11) \quad \det(M - \lambda I) = \begin{vmatrix} 2a_1x_{0,1} + a_2 - \lambda & a_3 \\ 2b_1x_{0,1} + b_2 & -\lambda \end{vmatrix} = 0$$

Boundary of the stable scope which is restricted by the coefficients is showed in.

$$(12) \quad |\lambda_{0,1}| = \frac{1}{2} [(2a_1x_{0,1} + a_2) \pm \sqrt{(2a_1x_{0,1} + a_2)^2 + 4(2a_3b_1x_{0,1} + a_3b_2)}] = 1$$

In some cases, the relationship between Δt_{n+1} and q_n is almost proportional. Therefore, the quadratic coefficient is closed to zero, and the fixed points $x_{0,1}$ are given by (13).

$$(13) \quad x_{0,1} = \frac{\pm(1 - a_3b_2) - a_2}{2a_1}$$

If $|b_2| < 1$, this iterative mapping has a contraction area, which means that the area of the mapping would be contracted by $|\det(M^*)|$ times after once iteration (Here M^* is the Jacobian Matrix as mentioned in Sec.2.1). If $\det(M^*) < 0$, the direction of the boundary would be changed after once iteration.

The results of corona discharge time series ($q-t$) under the conditions $|\lambda_{0,1}|=0.95$, $|\lambda_{0,1}|=1.13$ and $|\lambda_{0,1}|=1.26$, are calculated by using the 2D dynamic model, respectively, as shown in Fig. 5. When $|\lambda_{0,1}|$ is less than 1, the iterative $q-t$ series are regular and stable. On the contrary, when $|\lambda_{0,1}|$ is more than 1, the iterative results become disorder and unstable, and sensitive to the initial value of iteration. The time series ($q-t$) output by the model when $|\lambda_{0,1}|=1.13$ is similar to the most actual corona time series. This simulation could be regarded as a process from ordered to chaotic with variation of external conditions.

Table 1. Fitting results by using experimental data points (a. condition)

b_1		b_2		b_3		a_1		a_2		a_3		a_4		Adj. R-Square	
Value	S.E.	Value	S.E.	Value	S.E.	Value	S.E.	Value	S.E.	Value	S.E.	Value	S.E.	f	g
0.451	0.095	-0.413	0.055	0.204	0.006	-0.523	0.091	0.211	0.048	0.204	0.010	0.973	0.008	0.853	0.722

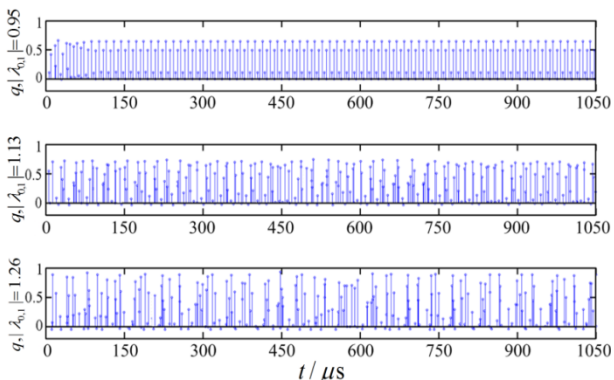


Fig.5. The corona time series ($q-t$) under different conditions: $|\lambda_{0,1}|=0.95$, $|\lambda_{0,1}|=1.13$ and $|\lambda_{0,1}|=1.26$.

B. Chaos bifurcations caused by change of parameters of the model system:

As for the nonlinear dynamic system, the transition from being regular to chaotic is essentially caused by the change of parameters of this system, which is represented as the change of experimental conditions on the microscopy, i.e., the gap distance, applied voltage value, atmospheric humidity. In order to analyze this transition, the chaotic maps which describe the variations of x (or q) with the parameters of the model, are discussed in this section.

Fig. 6(a). shows the influence of a_1 on the stability of the system. When a_1 is greater than zero, the iterative result tends to infinity. The first bifurcation appears when a_1 decreases to -1.116. With the further decrease of a_1 , the second and the third bifurcation occurs when $a_1=-1.823$ and -2.007, respectively. When a_2 decreases to about -2.172, the system evolves into chaos.

Fig. 6(b). shows the variation of x with a_2 . The system keeps stable until a_2 increases to 0.8412 while the first bifurcation occurs during the iteration. Since then, the second and the third bifurcation occur when a_2 increases to 1.121 and 1.221, respectively. And these bifurcations make the system evolve into the 4-periodical region and 8-periodical region, respectively. When a_2 increases to about 1.235, the system evolves into chaos completely. Similarly, the variation of the chaos dynamic characteristic caused by change of a_4 is showed in Fig. 6(c).

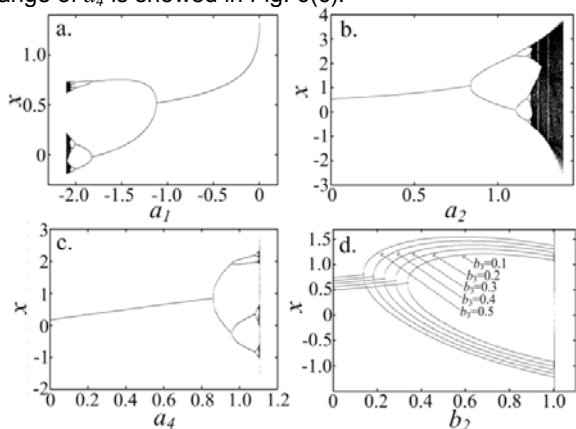


Fig.6. Chaotic maps of model system with variations of different coefficients

a. $a_1-x(a_2=0.211, a_3=0.973, a_4=0.562, b_1=0.451, b_2=-0.413, b_3=0.204)$;

b. $a_2-x(a_1=-0.52, a_3=0.973, a_4=0.562, b_1=0.451, b_2=-0.413, b_3=0.204)$;

c. $a_4-x(a_1=-0.523, a_2=0.211, a_3=0.973, b_1=0.451, b_2=-0.413, b_3=0.204)$;

d. $a_3b_2-x(a_1=-0.6, a_2=0.1, a_3=1, a_4=0.6, b_1=0.1)$

The coefficients b_1 and b_2 are determined by the relationship between Δt_{n+1} and q_n . If the relationship of Δt_{n+1} and q_n is supposed to linearity, the model has the feature of Henon map [19] which is irreversible and can be seen as the Poincare map of some three dimensional flows. In this case, the area of this map is gradually reduced by iterative steps when $|a_3b_2|<1$. When a_3 is set as 1.0, the effect of variation of b_2 under different value of b_3 is showed in Fig. 6(d). It indicates that the first bifurcation point shift left with increase of b_3 . But the instable point of a_3b_2 , which would make the iterative result tend to infinity, is unchanged yet.

C. Chaotic attractors:

The chaotic behavior takes place on an attractor when the dynamic system evolves into an unstable region. Chaotic attractor could be visualized by starting with a point in the basin of attraction of the attractor and then simply plot its subsequent orbit, as shown in Fig. 7. It is revealed that if and only if the fixed points $q_{0,1}$ are in range of (-0.225, 0), the dynamic system is stable. Therefore, the model will have some chaos due to the positive initial values of corona pulse ($q>0$) magnitude. Fig. 7(a) and (d) shows the chaos attractor mappings ($x-y$, by 104 times iterations) when a_4 was set to 0.918 and 0.959, respectively.

Fig. 7(b) and (c) are the local details of Fig. 7 (a). It is suggested that the attractors have the Henon self-similar structures in shape, and they have many stable periodic tracks exist in iteration process with a start of a valid initial value above zero. With the increase of a_4 , the contraction distortion of the chaos attractor will occur.

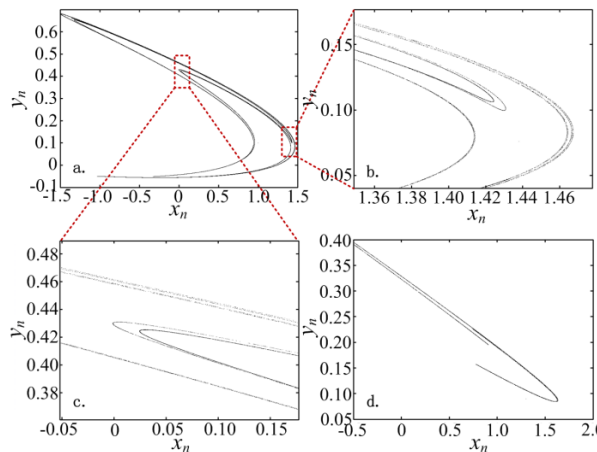


Fig.7. The $x-y$ attractors of the system by 104 times iterations

a. $a_4=0.918, a_1=-1.018, a_2=0.244, a_3=0.924, b_1=0.102, b_2=0.253, b_3=0.112$

b. $a_4=0.918, a_1=-1.018, a_2=0.244, a_3=0.924, b_1=0.102, b_2=0.253, b_3=0.112$ (detail figure)

c. $a_4=0.918, a_1=-1.018, a_2=0.244, a_3=0.924, b_1=0.102, b_2=0.253, b_3=0.112$ (detail figure)

d. $a_4=0.959, a_1=-1.018, a_2=0.244, a_3=0.924, b_1=0.102, b_2=0.253, b_3=0.112$

Conclusions

In this paper, a 2D nonlinear discrete dynamic model has been built for investigating the chaotic behavior driven by systematic component in corona discharge in air under DC voltage. According to the analysis and mathematic simulation, several conclusions are summarized as follows:

It is found that the distributions of points $(\Delta t_n, q_{n+1})$ and points $(q_n, \Delta t_n, q_{n+1})$ are very sensitive to the experiment condition. By using the valid statistical data, the specific form and its coefficients of the model were verified. Through plotting the chaos mappings, it is found the model system evolves from stable to chaotic with the variation of MLE (λ) which is caused by the changes of coefficients of the model functions. According to analysis and relevant simulation, it indicated that when $|\lambda|$ is less than 1, the $q-t$ series are stable and ordered after a few iterations starting with the arbitrary initial value; yet when $|\lambda|$ is more than 1, the $q-t$ series begin to be unstable and disorder during the iteration. The attractors of the model system have self-similar structures and its orbit shows a shrinkage process with the increase of a_d value.

REFERENCES

- [1] Morcos M M and Srivastava K D, Particle-initiated corona as indicative diagnosis in gas insulated systems, *Acta Physica Hungarica*, 68(1990), No. 1-2, 3-12
- [2] Lloyd, John R and Hess, Sonja, A corona discharge initiated electrochemical electrospray ionization technique, *Journal of the American Society for Mass Spectrometry*, 20(2009), NO.11, 1988-1996
- [3] White H J, Industrial electrostatic precipitation, *Addison-Wesley*, Reading, England, Chap 4 (1963)
- [4] Moore A D, Electrostatic and its applications *John Wiley & Sons*, New York, 3(1973)
- [5] Loeb L B, Electrical coronas Their Basic Physical Mechanisms, *University of California Press*, Berkeley, 1965, 1-15
- [6] Lilienfeld and Pedro, Stratospheric altimeter based on the density dependence of a corona discharge in air, *Review of Scientific Instruments*, 36 (1965), No. 7, 979-982
- [7] Robinson and Myron, Critical pressures of the positive corona discharge between concentric cylinders in air, *Journal of Applied Physics*, 40(1969), No. 13, 5107-5112
- [8] Loeb L B and Kip A F, Electrical discharges in air at atmospheric pressure The nature of the positive and negative point to plane coronas and the mechanism of spark propagation, *Journal of Applied Physics*, 10(1939), No.142, 142-160
- [9] Fitzsimmons K E, Threshold field studies of various positive corona phenomena, *Physical Review*, 61(1942), No. 3-4, 175-182
- [10] Trichel G W, The mechanism of the negative point to plane corona near onset, *Physical Review*, 54(1938), No. 12, 1078-1084
- [11] Loeb L B, Kip A F, Hudson G G, and Bennett W H, Pulses in negative point-to-plane corona, *Physical Review*, 60(1949), No. 10, 714-722
- [12] Ijumba N M, Lekganyane M and Britten A C, Comparative studies of DC corona losses in a corona cage and a point-plane gap, *AFRICON*, 2007, 1-7
- [13] Dissado L A, Suzuoki Y, and Kaneiwa H, Nagoya Proceedings of the Seventh International Conference on Properties and Applications of Dielectric Materials, 2003, 871-874
- [14] Tan X Y, Zhang Q G, Wang X H, et al., Chaotic characteristics of corona discharges in atmospheric air, *Journal of Applied Physics*, 104(2008), No.10, 103309-103318
- [15] Luo Y F, Ji H Y, Huang P, Li Y M, Chaotic characteristic of time series of partial discharge in oil-paper insulation, *Plasma Science and Technology*, 13(2011), No.6, 740-746
- [16] Fromm U, Interpretation of partial discharges at DC voltages, *IEEE transactions on Dielectrics and Electrical Insulation*, 2(1995), No. 5, 761-770
- [17] Hayakawa N, Hatta K, Okabe S, et al., Streamer and leader discharge propagation characteristics leading to breakdown in electronegative gases, *IEEE transactions on Dielectrics and Electrical Insulation*, 13(2006), NO. 4, 842-849
- [18] Hayakawa N, Yoshitake Y, Koshino N, et al., Impulse partial discharge characteristics and their mechanisms under non-uniform electric field in N₂/SF₆ Gas mixtures, *IEEE transactions On Dielectrics and Electrical Insulation*, 12(2005), No. 5, 1035-1042
- [19] Henon M, A two-dimensional mapping with a stranger attractor Communications in, *Mathematical Physics*, 50(1976), No. 1, 69-77

Authors: PHD student Ren Ming, High Voltage Division, School of Electrical Engineering, Xi'an Jiaotong University, China, 710049, E-mail: ren.ming@stu.xjtu.edu.cn;
Dr. Dong Ming, High Voltage Division, School of Electrical Engineering, Xi'an Jiaotong University, China, 710049, E-mail: dongming@mail.xjtu.edu.cn;
PHD student Ren Zhong, High Voltage Division, School of Electrical Engineering, Xi'an Jiaotong University, China, 710049, E-mail: the.moment1989@stu.xjtu.edu.cn;
Prof. Qiu Ai Ci, School of Electrical Engineering, Xi'an Jiaotong University, China, 710049 & Northwest Institute of Nuclear Technology of China, Xi'an, China, 710049, E-mail: qiuac@mail.cae.ac.cn.